Silver Nanoprisms Acting as Multipolar Nanoantennas under a Low-Intensity Infrared Optical Field Exciting Fluorescence from Eu3+

ARTICLE *in* JOURNAL OF PHYSICAL CHEMISTRY LETTERS · OCTOBER 2013

Impact Factor: 7.46 · DOI: 10.1021/jz4019354

4 AUTHORS:

Zubair Buch
Monash University (Australia)
5 PUBLICATIONS **16** CITATIONS
SEE PROFILE

Vineet Kumar
North Carolina State University
12 PUBLICATIONS **36** CITATIONS
SEE PROFILE

Hitesh Mamgain
WITec Wissenschaftliche
12 PUBLICATIONS **97** CITATIONS
SEE PROFILE

Santa Chawla
National Physical Laboratory - India
92 PUBLICATIONS **790** CITATIONS
SEE PROFILE

THE JOURNAL OF PHYSICAL CHEMISTRY Letters

Letter

pubs.acs.org/JPCL

Silver Nanoprisms Acting as Multipolar Nanoantennas under a Low-Intensity Infrared Optical Field Exciting Fluorescence from Eu^{3+}

Zubair Buch,[†] Vineet Kumar,[†] Hitesh Mamgain,[‡] and Santa Chawla*,[†]

[†]Luminescent Materials Group, CSIR-National Physical Laboratory, Dr. K.S. Krishnan Road, New Delhi 110012, India

[‡]WITec GmbH, Lise-Meitner-Strasse, 6 D-89081 Ulm, Germany

Supporting Information

ABSTRACT: A silver nanoprism (Ag NP) generates a near field due to multipolar surface plasmon resonance (SPR) and lightening rod effects and acts as a multipolar nanoantenna. The ability of Ag NPs to create such an effect even under an infrared (IR) optical field far off of resonance from the SPR frequency is demonstrated through finite difference time domain simulations of exact Ag NPs and hybrids. The conclusive experimental proof of such a near field around Ag NPs under low-intensity (1.5 mW) IR (980 nm) light came when it could excite fluorescence from YVO_4/Eu^{3+} nanoparticles that otherwise do not fluoresce under IR. The results open up new vistas for exclusive plasmonic excitation of fluorescence through metal NP hybrids/ensembles.

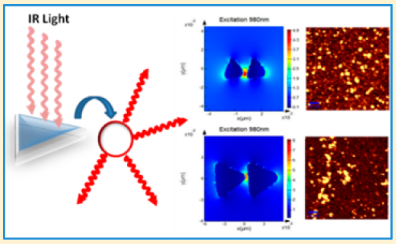

SECTION: Plasmonics, Optical Materials, and Hard Matter

Noble metal nanoparticles (MNPs) have exceptional capability to design the near field in response to incident light according to their shape and size. Local field enhancement in subwavelength MNPs is caused due to two major reasons, (i) collective oscillation of free surface electrons, known as surface plasmon resonance (SPR), and (ii) a lightening rod effect, which is purely a geometric phenomenon and depends only on the shape of the metal nanostructure.[1] Due to such effects, noble MNPs behave as nanoantennas that enhance the incoming electromagnetic (EM) radiation. One important manifestation of such a phenomenon is metal-enhanced fluorescence, which has promising applications in solar cells, solid-state lighting, bioimaging, and so forth.[2,3] The enhancement of fluorescence is credited to the highly localized EM fields, which generate in the near field of plasmonic nanostructures upon excitation by incident light of suitable frequency. Many reports have demonstrated fluorescence enhancement by placing the fluorophore in close vicinity of MNPs;[4,5] however, a physical contact between the two can lead to fluorescence quenching by favoring nonradiative transitions from the fluorophore.[6] Existing knowledge of MNP-enhanced fluorescence suggests that fluorescence enhancement can be realized by two methods, namely, (i) excitation enhancement and (ii) emission enhancement. The absorption or emission band of the fluorophores must overlap with the SPR of the MNP to obtain efficient excitation or emission enhancement while maintaining the excitation light source in resonance with the SPR band of the MNP.[4,7−9] Our previous study on YVO_4/Eu^{3+} NPs conjugated with silver nanoprisms (Ag NPs) also exhibited fluorescence enhancement through excitation enhancement.[10] In all such studies on MNP-enhanced fluorescence, direct excitation of the fluorophore has taken place in addition to energy transfer from the excited MNP to fluorophore. The plasmonic near field as the sole source of excitation of the fluorophore has never been explored before.

In this Letter, we explore the multipolar character of silver nanoprisms and employ it for realizing unprecedented plasmonic excitation of fluorescence from the YVO_4/Eu^{3+} nanophosphor at off-resonance excitation frequency in the IR region. To ascertain the role of the local field in exciting fluorescence, we chose incident laser light of 980 nm as it cannot excite the fluorophore directly. Silver nanoprisms were chosen due to their ability to exhibit distinct multipolar resonances and a lightening rod effect, which results in generation of highly localized EM fields with enhancement factors $|E|^2$ reaching more than 100 fold.[11,12] The fluorophore of choice are NPs of rare earth (Eu^{3+})-doped YVO_4 that is a proven high-efficiency down-conversion phosphor excitable by ultraviolet (UV) light,[13] which rules out the possibility of its direct excitation by 980 nm light. The studied MNP−nanophosphor integrated material system is comprised of a thin film of YVO_4/Eu^{3+} NPs and a layer of silver nanoprisms separated by a thin spacer layer of polyvinyl alcohol (PVA) to avoid direct contact of both species. The integrated material system is excited by 980 nm IR laser, which is far from the excitation and emission spectrum of YVO_4/Eu^{3+} NPs, thus ensuring direct observation of the influence of enhanced EM fields generated in the near field of Ag nanoprisms on the nanophosphor. Confocal fluorescence microscopy has been employed to study fluorescence from YVO_4/Eu^{3+} NPs placed in the proximity of silver nanoprisms. We observe an unusual phenomenon of fluorescence emission from a fluorophore−Ag

Received: September 9, 2013
Accepted: October 30, 2013

   dx.doi.org/10.1021/jz4019354 | J. Phys. Chem. Lett. 2013, 4, 3834−3838

nanoprism combine under very low IR excitation (980 nm, 1.5 mW). To understand the occurrence of fluorescence, local field studies of exact silver nanoprisms used in the experiment were carried out through finite difference time domain (FDTD) simulation under 980 nm optical excitation, and a cause−effect relationship was established.

NPs of YVO_4 doped with Eu^{3+} (5 atomic %) were synthesized using a coprecipitation method at room temperature.[14] Characterization through XRD and TEM confirm formation of monophasic (tetragonal) transparent spherical NPs of YVO_4/Eu^{3+} of average size 5 nm. Silver nanoprisms were synthesized by the wet chemical route by optimizing the method developed by V. E Torres Heredia.[15] Two different samples were synthesized with average edge lengths of the nanoprisms of (i) 22 and (ii) 45 nm, as confirmed by TEM images. Thin films were made by first spin coating a thin layer of YVO_4/Eu^{3+} NPs dispersed in ethanol on a clean glass microscope coverslip followed by overcoating a thin (~few nm) spacer layer made of 3% PVA in aqueous solution. A colloidal solution of Ag nanoprisms was then spin-cast on top of the PVA layer. Optimized and uniform coating parameters were used for all of the samples throughout the experiment. Thin films of YVO_4/Eu^{3+} NPs combined with Ag nanoprisms were examined under a confocal microscope (WITec R 300) with N.A. = 0.9 and an IR diode laser (output wavelength 980 nm, power 1.5 mW) as the exciting source.

Confocal fluorescence images of different samples (Figure 1i−iii) and corresponding emission spectra (integrated intensity) when excited by 980 nm light are shown in Figure 1vi. Figure 1iv shows the collage of TEM images of silver nanoprisms of average edge lengths of 22 (a1−a3) and 45 nm (b1−b3) with different degrees of truncation. The schematic arrangement of the thin film prepared for confocal measurements is shown in Figure 1v. From the confocal image of thin film of only YVO_4/Eu^{3+} NPs (Figure 1i) and corresponding integrated intensity spectra (Figure 1vi), it is conspicuous that no emission from YVO_4/Eu^{3+} takes place when excited by 980 nm light. In contrast, the confocal images of YVO_4/Eu^{3+} in proximity with Ag nanoprisms with average edge lengths of 22 (Figure 1ii) and 45 nm (Figure 1iii) clearly show regions of bright fluorescence, and the corresponding emission spectra (Figure 1vi) confirm the emission from YVO_4/Eu^{3+} with peaks at 615 and 619 nm, the signature emission of Eu^{3+} due to the $^5D_0-^7F_2$ transitions. The fluorescence spectra and confocal image of YVO_4/Eu^{3+} combined with 45 nm Ag nanoprisms exhibit much greater intensity. Hence, it is clear from emission spectra of both samples that the fluorescence observed corresponds to the characteristic electric dipolar transitions of Eu^{3+} ions, which confirms emission under 980 nm IR excitation from the fluorophore (YVO_4/Eu^{3+}) solely due to their propinquity to Ag nanoprisms.

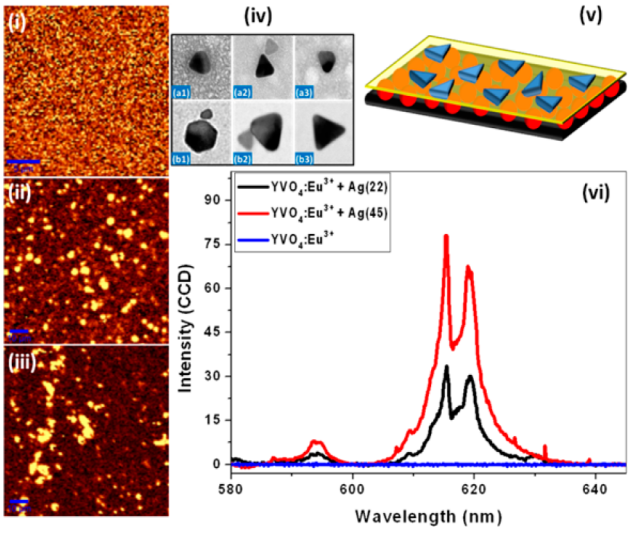

Figure 1. Confocal fluorescence image of thin films of (i) YVO_4/Eu, (ii) YVO_4Eu + 22 nm Ag nanoprism combined, and (iii) YVO_4/Eu + 45 nm Ag nanoprism combine, (iv) TEM images of Ag nanoprisms of 22 (a1,a2,a3) and 45 nm (b1,b2,b3), (v) schematic of arrangements of YVO_4Eu NPs (red spheres), the PVA layer (yellow transparent layer), and Ag NPs (blue prisms) in thin films used for the confocal fluorescence study, and (vi) integrated fluorescence spectra of the samples under 980 nm laser excitation taken by confocal fluorescence measurements.

The local field generated by silver nanoprisms and its implications in inducing fluorescence were studied by performing three-dimensional FDTD simulations of exact silver nanoprisms (imported from a transmission electron micrograph), one nanoprism geometry taken from each sample on the basis of the average distribution. The FDTD technique is considered very suitable for plasmonic simulations, and in this technique, both electric $E(t)$ and magnetic $H(t)$ components of the EM field are made discrete in time. The simulation is then run to solve Maxwell's equations in $E(t)$ and $H(t)$, and the steady-state continuous wave field $E(\omega)$ is calculated from $E(t)$ by Fourier transform during the simulation, and each simulation gives broad-band results.

$$E(\omega) = \int_0^T e^{i\omega t} E(t)\, dt$$

TEM images of Ag nanoprisms with edge lengths of (i) 45 and (ii) 22 nm were imported for FDTD analysis. Simulations were performed by using FDTD solutions (version 8.5).[16] The mesh size taken was 0.8 nm, which returns more accurate results than the discrete dipole approximation (DDA).[11] The material response for the Ag nanoprism was taken from Palik,[17] which corresponded well with the FDTD model for the chosen frequency range (Supporting Information Figure S1), and the field was allowed to evolve for 200 fs.

We measured the absorption spectra of Ag nanoprisms by UV−visible spectroscopy (Figure 2iii,iv) and calculated their extinction spectrum by the FDTD method, as shown in Figure 2i,ii. FDTD simulations were done conforming to the experimental setup used for confocal measurements, and light was injected from the Z axis, falling perpendicularly on the nanoprism surface and passing through them. Silver nanoprisms of 22 and 45 nm edge lengths were individually studied followed by their dimers and trimers. During spin coating, many aggregates of Ag NPs are formed, which leads to plasmonic coupling between adjacent nanoprisms. This coupling between multiple Ag nanoprisms was simulated by arranging nanoprism dimers and trimers as a linear array in similar orientation with a typical separation of 5 nm between two adjacent nanoprisms. The main extinction peaks for a single Ag nanoprism with edge lengths of 22 and 45 nm were observed at 400 and 430 nm, respectively. When a second nanoprism was added at a distance of 5 nm, the extinction spectrum red shifted for both types of nanoprisms. Addition of a third nanoprism further red shifted the extinction spectrum (Figure 2i,ii). A trend of red shifting as well as broadening of

dx.doi.org/10.1021/jz4019354 | J. Phys. Chem. Lett. 2013, 4, 3834−3838

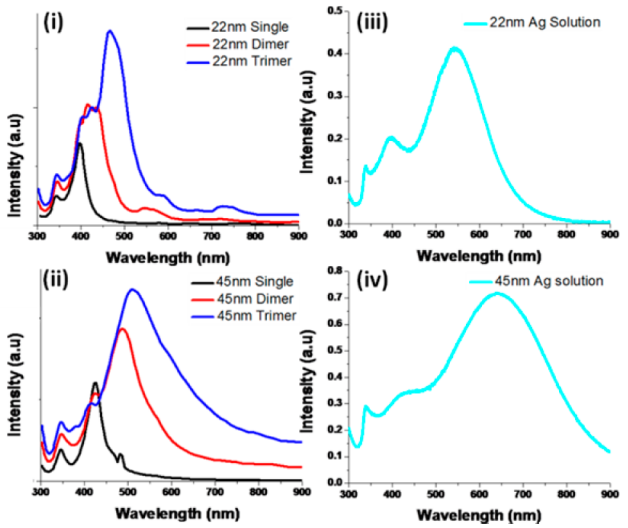

Figure 2. Extinction spectra of an exact Ag nanoprism, single, dimer, and trimer with edge lengths of 22 (i) and 45 nm (ii) in an aqueous environment by FDTD simulation with *Z* as the injection axis; the experimental UV−visible absorption spectra of the corresponding Ag NP colloidal aqueous solution (iii, iv).

extinction spectra for a multitude of Ag NPs thus became apparent. The major reason believed for such changes is the interaction of localized surface plasmons of the adjacent nanoprisms and interference of the EM fields generated by them.[18,19] Experimentally measured UV−visible absorption spectra of silver nanoprism colloidal solutions (Figure 2iii,iv) indicate a much broader peak that red shifts with an increase in the Ag NP edge length (540 and 635 nm for 22 and 45 nm, respectively). These broad peaks emerge as a result of the inhomogeneous damping due to the random spatial position and orientation of silver nanoprisms in the colloidal solution, giving different peaks (see Supporting Information Figure S2), and the broad curve in UV−visible spectra can be understood as a convolution of all resulting peaks together. Also, broadening of absorption spectra (experimental) and extinction spectra (FDTD calculation) for larger edge length Ag NPs suggests spreading of the conduction electrons over a larger surface area, which lessens the restoring force experienced by them when displaced by an EM field.[20]

In addition to the main dipolar peak shown in the extinction spectrum, a small shoulder peak appears at around 340 nm for nanoprisms of both sizes, present in FDTD as well as the UV−visible spectra. The position of this peak is independent of the size and multiplicity of the nanoprisms, and it can be assigned as the out-of-plane quadrupolar resonance.[11]

The EM enhancement $L(\nu)$ results due to SPR in silver nanoprisms and is equivalent to $L_{SPR}(\nu)L_{LR}$, where $L_{SPR}(\nu)$ is the local field associated with the plasmon excitation at incident frequency "ν" and L_{LR} is the lightening rod effect. The SPR in the MNP changes upon variations in size, shape, or dielectric environment of the NP, and the main resonance peaks of the silver nanoprism can be estimated from their extinction spectra (Figure 2). However, when plotting E-field contours of plasmonic nanostructures, some deviations in spectral positions of surface-averaged E-field enhancement are possible from the extinction spectrum.[21] There occurs a shift between the near- and far-field energies of plasmons that causes this deviation,[22] which can also occur for interacting hybrids.[23] For estimation of these EM enhancements, we calculated the local field generated by Ag NPs by the FDTD method. The EM enhancement arising due to the silver nanoprism and ensembles has clear implications for causing nonlinear effects also because subwavelength particles are independent of phase-matching considerations for nonlinear effects.[24] Thus, a randomly arranged ensemble of Ag NPs on our thin film system is likely to exhibit nonlinear processes leading to emission of incoherent signals in all directions. Local electric field enhancements $|E|^2$ were calculated for frequencies corresponding to SPR of Ag NPs; the emission wavelength of Eu^{3+} (615 nm) and the incident wavelength (980 nm) for a quantitative comparison are presented in Table 1. FDTD simulation of exact Ag NPs

Table 1. Field Enhancement of Ag Nanoprisms at Different Excitation Frequencies

	E-Field Enhancement $|E|^2$ (Z-Direction)			
	SPR	615 nm	980 nm	
Ag NP edge length	single NP	single NP	single NP	dimer
22 nm	260	12	10	30
45 nm	648	39	50	152

under 980 nm excitation reveals that the field enhancement $|E|^2$ reaches 10 times the applied field for a single 22 nm edge length Ag NP and 30 times for a dimer (Figure 3). In the case

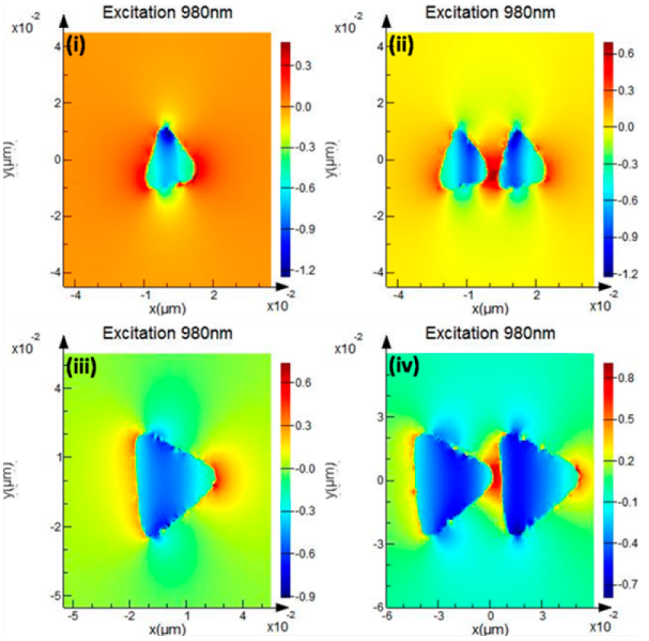

Figure 3. Optical properties of single Ag nanoprisms and dimers calculated by the FDTD method by importing the exact TEM image of the Ag NP. Near-field image of a Ag nanoprism for a (i) 22 nm single NP, (ii) 22 nm Ag dimer with 5 nm separation, (iii) 45 nm single NP, and (iv) 45 nm dimer with 5 nm separation. All images are shown on a log scale.

of the 45 nm edge length Ag NP, $|E|^2$ enhancement of 50 times is obtained for a single Ag NP, which becomes 152 times for a dimer. The Au spheroid (25 nm) also exhibited $|E|^2$ enhancement (10 times) under 850 nm light, off resonance from SPR (500 nm).[25] For both Ag nanoprism samples, the separation between two Ag NPs in a dimer was kept at 5 nm approximately. We considered this distance convenient for

dx.doi.org/10.1021/jz4019354 | J. Phys. Chem. Lett. 2013, 4, 3834−3838

understanding the change in the enhancement values $|E|^2$ as we move from monomer to dimer (Figure 3).

It is evident from these results that the $|E|^2$ factor multiplies approximately 3-fold for a dimer, and hence, larger enhancements are expected for bigger ensembles of Ag NPs. These large enhancements are credited to the ability of metal NP dimers and aggregates to confine incident light around themselves and in the gaps between them, giving rise to heightened EM fields in their near-field region.[26]

The FDTD simulation results of exact Ag NPs under a 980 nm optical field unequivocally establish generation of a significant EM field around Ag nanoprisms with energy corresponding to the plasmon frequency. A direct correlation of this is experimentally realized when such an EM field excites the fluorescence of Eu^{3+} doped in NPs of YVO_4 (Figure 1vi).

The scheme for energy transfer from Ag nanoprisms to Eu^{3+} levels is indicated in the energy level diagram (Figure 4). The

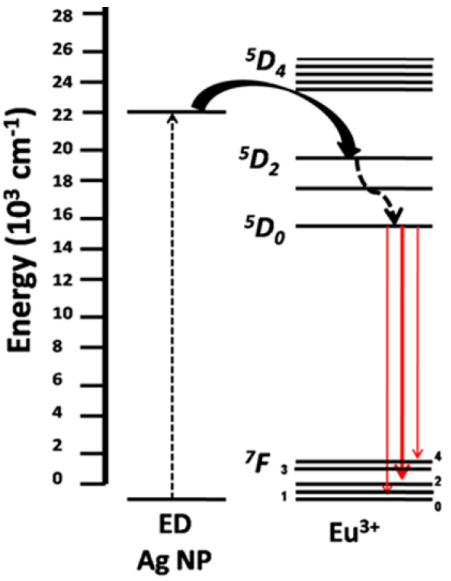

Figure 4. Energy level diagram showing excitation of a Ag NP and subsequent energy transfer to Eu^{3+} levels leading to red fluorescence emission.

minimum energy required for direct excitation of Eu^{3+} from its ground state $^7F_0$ to the $^5D_1$ level corresponds to a wavelength of about 525 nm (approx), and this energy is much higher than the incident infrared light at 980 nm, which thus cannot excite fluorescence from YVO_4/Eu^{3+} NPs, as is evidenced from Figure 1. For the Ag NP conjugated YVO_4/Eu^{3+} thin film system, the silver nanoprisms act as nanoantennas that store the incident energy (980 nm) in their localized plasmon mode corresponding to their extinction spectra (Figure 2), which is suitable for exciting Eu^{3+} ions.

In addition, nonlinear effects due to MNP ensembles can also contribute toward the fluorescence excitation of YVO_4/Eu^{3+} by second- and higher-harmonic generations of incident IR frequency. The generated near field around Ag NPs excites the neighboring Eu^{3+} ions to the ^5D_J levels followed by relaxation through phonons to the bottom $^5D_0$ level. Very efficient radiative transition from the lowest $^5D_0$ excited level to lower ^7F_J levels gives rise to sharp emission peaks in the red spectral region (Figure1vi); the strongest emission corresponds to the $^5D_0-^7F_2$ electric dipole transition. Because the scattering spectra of Ag NPs do not overlap with the emission wavelength of Eu^{3+}, no emission enhancement takes place. As SPR energy modes cover the excitation band of the fluorophore (Figure 2), the generated near field of Ag NP becomes the sole excitation source for Eu^{3+}.

In summary, we have shown that the EM field generated near silver nanoprisms under IR light is the sole excitation source for YVO_4/Eu^{3+} NPs, which otherwise cannot be excited by IR light. This is direct excitation of the fluorophore through a plasmonic optical field under an incident frequency far off-resonance from SPR of silver nanoprisms. Our results bring new insight to engineer fluorescence excitation and enhancement by the local EM field of MNPs and thus manifest tremendous potential in broad areas of plasmonics, fluorescence, and related applications such as plasmonic photovoltaics, optical sensing, bioimaging, and so forth.

EXPERIMENTAL SECTION

Sample Synthesis. Ag nanoprisms were synthesized from $AgNO_3$, polyvinyl pyrrolidone solution, and trisodium citrate in an aqueous medium. Tuning the sizes of nanoprisms was achieved by adding varied quantities of $NaBH_4$ solution with different concentrations of H_2O_2 solution (30% W/V). NPs of $Y_{0.95\%}VO_4/(Eu)_{0.05\%}$ was synthesized using a coprecipitation method by using nitrate precursors in an alkaline solution with pH 10. TEM images showed near-spherical particles of average size 5 nm.

Confocal Fluorescence Measurements. A confocal microscope (WITec R 300) was used to observe the fluorescence emission from a prepared thin film under IR light. A high-throughput lens-based spectrograph (UHTS 300) with a 300 mm focal length, connected with a Peltier-cooled back-illuminated CCD camera with better than 90% QE in the visible excitation, was employed for data collection.

FDTD Simulation. The near-field and extinction properties of silver nanoprisms and hybrids were calculated by the FDTD method (Lumerical FDTD solutions 8.5). The refractive index of the surrounding medium was kept at 1.33. We used the Conformal Variant 1 mesh refinement option, and standard PML boundaries were used to prevent reflections from absorbing boundaries. We used a broad-band total field scattering field (TFSF) source and implemented suitable monitors to calculate the near-field and extinction properties of silver nanoprisms. A plane wave source as the incident optical field was injected from *Z*- axis, falling perpendicularly on silver nanoprisms resting on a plane, and this configuration exactly conforms to the setup used for confocal fluorescence measurements.

ASSOCIATED CONTENT

Supporting Information

Real and imaginary parts of the dielectric function of silver (Figure S1) and the absorption and scattering spectrum of silver nanoprisms calculated by injecting incident light from *X*, *Y*, and *Z* directions (Figure S2). This material is available free of charge via the Internet at http://pubs.acs.org.

AUTHOR INFORMATION

Corresponding Author

*E-mail santa@nplindia.org.

Notes

The authors declare no competing financial interest.

■ ACKNOWLEDGMENTS

The authors thank Mithun Bhomkar of Lumerical Solutions for his valuable advice regarding FDTD simulation.

■ REFERENCES

(1) Maier, S. A. *Plasmonics: Fundamentals and Applications*; Springer: New York, 2007; p *162*.
(2) Geddes, C. D.; Lakowikz, J. R. Metal Enhanced Fluorescence. *J. Fluoresc.* **2002**, *12*, 121−129.
(3) Atre, A. C.; Etxarri, A. G.; Alaeian, H.; Dionne, J. A. Towards High Efficiency Solar Upconversion with Plasmonic Nanostructures. *J. Opt.* **2012**, *14*, 1−7.
(4) Wang, Q.; Song, F.; Lin, S.; Liu, J.; Zhao, H.; Zhang, C.; Ming, C.; Pun, E. Y. B. Optical Properties of Silver Nanoprisms and Their Influence on Fluorescence of Europium Complex. *Opt. Express* **2011**, *19*, 6999−7006.
(5) Feng, W.; Sun, L. D.; Yan, C. H. Ag Nanowires Enhanced Upconversion Emission of $NaYF_4$:Yb:Er Nanocrystals via a Direct Assembly Method. *Chem. Commun.* **2009**, 4393−4395.
(6) Anger, P.; Bharadwaj, P.; Novotny, L. Enhancement and Quenching of Single-Molecule Fluorescence. *Phys. Rev. Lett.* **2006**, *96*, 1−4.
(7) Wang, Q.; Song, F.; Lin, S.; Ming, C.; Zhao, H.; Liu, J.; Zhang, C.; Pun, E. Y. B. Effect of Silver Nanoparticles of Different Shapes on Luminescence of Samarium Complex at Two Different Excitation Wavelengths. *J. Nanopart. Res.* **2011**, *13*, 3861−3865.
(8) Chen, Y.; Munechika, K.; Ginger, D. S. Dependence of Fluorescence Intensity on the Spectral Overlap between Fluorophores and Plasmon Resonant Single Silver Nanoparticles. *Nano Lett.* **2007**, *7*, 690−696.
(9) Geddes, C. D. *Metal Enhanced Fluorescence*; Wiley, Hoboken, NJ, 2010; p 91.
(10) Buch, Z.; Kumar, V.; Mamgain, H.; Chawla, S. Silver Nanoprism Enhanced Fluorescence in YVO_4:Eu^{3+} Nanoparticles. *Chem. Commun.* **2013**, *49*, 9485−9487.
(11) Guedje, F. K.; Giloan, M.; Potara, M.; Hounkonnou, M. N.; Astilean, S. Optical Properties of Single Silver Triangular Nanoprism. *Phys. Scr.* **2012**, *86*, 1−6.
(12) Hao, E.; Schatz, G. C. Electromagnetic Field around Silver Nanoparticles and Dimers. *J. Chem. Phys.* **2004**, *120*, 357−366.
(13) Palilla, F. C.; Levine, A. K. YVO_4:Eu: A Highly Efficient, Red Emitting Phosphor for High Pressure Mercury Lamps. *Appl. Opt.* **1966**, *5*, 1467−1468.
(14) Kumar, V.; Khan, A.; Chawla, S. Intense Red-Emitting Doped Nanoparticles of YVO_4 for Spectral Conversion towards Improved Energy Harvesting by Solar Cells. *J. Phys. D: Appl. Phys.* **2013**, *46*, 1−9.
(15) Heredia, V. E. T. Doctoral Thesis, Universidad Politecnica de Catalunya, Barcelona, Catalonya, 2011.
(16) Lumerical Homepage. www.lumerical.com (2013).
(17) Palik, E. D. *Handbook of Optical Constants of Solids*; Elsevier Science and Tech: Baltimore, MD, 1998.
(18) Maier, S. A.; Brongersma, M. L.; Kik, P. G.; Atwater, H. A. Observation of Near-Field Coupling in Metal Nanoparticle Chains Using Far Field Polarization Spectroscopy. *Phys. Rev. B* **2002**, *65*, 1−4.
(19) Nordlander, P.; Oubre, C.; Prodan, E.; Li, K.; Stockman, M. I. Plasmon Hybridization in Nanoparticle Dimers. *Nano Lett.* **2004**, *4*, 899−903.
(20) Evanoff, D. D., Jr.; Chumanov, G. Synthesis and Optical Properties of Silver Nanoparticles and Arrays. *ChemPhysChem* **2005**, *6*, 1221−1231.
(21) Kelly, L.; Coronado, E.; Zhao, L. L.; Schatz, G. C. The Optical Properties of Metal Nanoparticles: The Influence of Size, Shape, and Dielectric Environment. *J. Phys. Chem. B* **2003**, *107*, 668−677.
(22) Zuloga, J.; Nordlander, P. On the Energy Shift between Near-Field and Far-Field Peak Intensities in Localized Plasmon Systems. *Nano Lett.* **2011**, *11*, 1280−1283.
(23) Schertz, F.; Schmelzeisen, M.; Mohammadi, R.; Kreiter, M.; Elmers, H. J.; Schonhense, G. Near Field of Strongly Coupling Plasmons: Uncovering Dark Modes. *Nano Lett.* **2012**, *12*, 1885−1890.
(24) Kauranen, M.; Zayats, A. V. Nonlinear Plasmonics. *Nat. Photonics* **2012**, *6*, 737−748.
(25) Atwater, H. A.; Polman, A. Plasmonics for Improved Photovoltaic Devices. *Nat. Mater.* **2010**, *9*, 205−213.
(26) Xu, H.; Bjerneld, E. J.; Kall, M.; Borjesson, L. Spectroscopy of Single Hemoglobin Molecules by Surface Enhanced Raman Scattering. *Phys. Rev. Lett.* **1999**, *83*, 4357−4360.